PHYSICS

Observation of a gravitational Aharonov-Bohm effect

Chris Overstreet[1]†, Peter Asenbaum[1,2]†, Joseph Curti[1], Minjeong Kim[1], Mark A. Kasevich[1]*

Gravity curves space and time. This can lead to proper time differences between freely falling, nonlocal trajectories. A spatial superposition of a massive particle is predicted to be sensitive to this effect. We measure the gravitational phase shift induced in a matter-wave interferometer by a kilogram-scale source mass close to one of the wave packets. Deflections of each interferometer arm due to the source mass are independently measured. The phase shift deviates from the deflection-induced phase contribution, as predicted by quantum mechanics. In addition, the observed scaling of the phase shift is consistent with Heisenberg's error-disturbance relation. These results show that gravity creates Aharonov-Bohm phase shifts analogous to those produced by electromagnetic interactions.

In classical physics, the state of a particle is given by its position and momentum. Because the trajectory of a classical particle is determined by its interactions with local fields, the deflection of a particle can be used to observe a field. However, a classical particle cannot measure the action along its trajectory.

The situation is different in quantum mechanics. As Aharonov and Bohm argued in 1959, a particle in a spatial superposition is sensitive to the potential energy difference between its wave packets even if the field vanishes along their trajectories (*1*). A matter-wave interferometer can therefore measure a phase shift due to the potential even if the interferometer arms are not deflected. This phase shift ϕ_{AB} is given by the action difference ΔS between arms according to the expression $\phi_{AB} = \Delta S/\hbar$ (*1*). The Aharonov-Bohm effect can be described in terms of a quantum particle interacting with a classical electromagnetic potential (*1*) or in terms of a quantum particle interacting locally with a quantized electromagnetic field and source (*2*).

The Aharonov-Bohm effect induced by a magnetic field was first observed in 1960 (*3*). Since then, experiments have identified related effects in a variety of systems (*4*, *5*). The successful observation of Aharonov-Bohm phase shifts in the electromagnetic domain raises a question: Can analogous phase shifts be caused by gravity as well? Quantum mechanics predicts that gravity can create an action difference between interferometer arms, giving rise to a "gravitational Aharonov-Bohm effect" (*6*). In general relativity, this phenomenon is described by the gravitationally induced proper time difference between the geodesics corresponding to the interferometer arm trajectories. This effect has not previously been observed. Its experimental detection in an atom interferometer was proposed in (*7*).

Prior experiments (*8*) were not sensitive to the gravitational Aharonov-Bohm effect because $\Delta S \approx 0$ when the wave packet separation is small compared to the length scale of the gravitational potential (*9*, *10*). The interferometer phase in this regime is proportional to the deflection of the atomic wave packet with respect to its beam splitters (*11*, *12*) and is independent of the particle mass m. However, when the wave packet separation is large, ΔS becomes nonzero. Qualitatively, an interferometer enters this nonlocal regime when the wave packet separation becomes larger than the distance between the source mass and an interferometer arm.

We use a light-pulse ^{87}Rb atom interferometer (*12*) with large–momentum-transfer beam splitters ($52\hbar k$, where k is the laser wave number) and large wave packet separation (25 cm) to measure the phase shift induced by a tungsten source mass. At its closest approach, one interferometer arm passes within 7.5 cm of the source mass, which alters its proper time (Fig. 1A). The source mass also deflects the interferometer arms. To quantify the influence of deflections on the phase shift, we measure the deflections with a pair of $4\hbar k$ interferometers (2-cm wave packet separation). The phase shift of the $52\hbar k$ interferometer deviates strongly from the deflection-induced phase contribution. We show that $\phi_{AB} \neq 0$, demonstrating the gravitational Aharonov-Bohm effect in this system.

In the experiment (*13*, *14*), a cloud of ^{87}Rb is evaporatively cooled to ~1 μK in a magnetic trap, magnetically lensed to a velocity width of 2 mm/s, and launched into a 10-m vacuum chamber at 13 m/s by an optical lattice. The lattice depth is decreased for a short interval during the launch to release half of the atoms at a lower velocity [see materials and methods for details (*15*)]. After the launch, the two clouds are decelerated to a relative momentum of $2\hbar k$ by sequential Bragg transitions and are used as the inputs of a single-source gradiometer (*16*) with baseline 24 cm (Fig. 1B). The matter-wave beam splitters and mirrors consist of laser pulses that transfer momentum to the atoms via Bragg transitions. The midpoint trajectory of each $4\hbar k$ interferometer is matched to the trajectory of one arm of the $52\hbar k$ interferometer. The $52\hbar k$, upper $4\hbar k$, and lower $4\hbar k$ gradiometers are implemented in separate shots. The upper interferometer in each gradiometer is sensitive to the source mass, whereas the lower interferometer mainly acts as a phase reference. This reference is necessary to remove contributions to the phase shift arising from fluctuations in the phase of the optical field. The time between the initial beam splitter pulse and the mirror pulse (interferometer time T) is

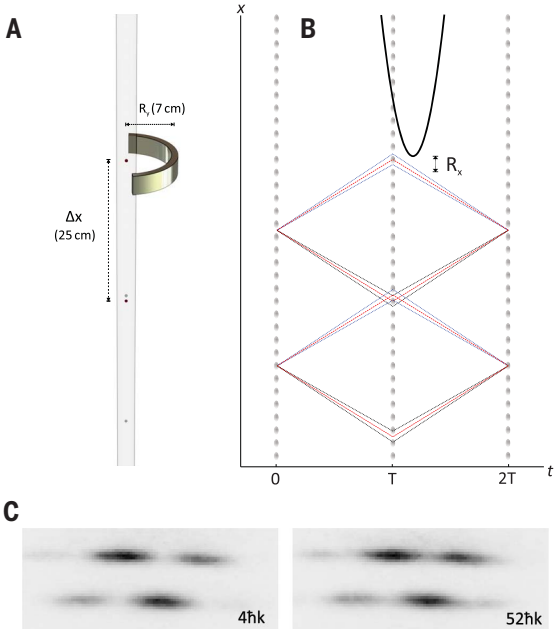

Fig. 1. Experimental setup. (**A**) Interferometer arms, tungsten source mass, and laser beam splitter. One arm of a light-pulse atom interferometer approaches the source mass, while the other arm remains far away. (**B**) Space-time diagram of gradiometer geometries in a freely falling reference frame. The red, blue, and black dotted lines represent the trajectories of the $52\hbar k$, upper $4\hbar k$, and lower $4\hbar k$ gradiometers, respectively, while the solid black line represents the trajectory of the source mass. Interferometer pulses (gray dashed lines) occur at times $t = 0$, $t = T$, and $t = 2T$. (**C**) Fluorescence images of interferometer output ports, $4\hbar k$ (left) and $52\hbar k$ (right).

[1]Department of Physics, Stanford University, Stanford, CA 94305, USA. [2]Institute for Quantum Optics and Quantum Information (IQOQI) Vienna, Austrian Academy of Sciences, Boltzmanngasse 3, 1090 Vienna, Austria.
*Corresponding author. Email: kasevich@stanford.edu
†These authors contributed equally to this work.

0.82 s. After a gradiometer sequence is complete, the atoms are imaged by resonant scattering (Fig. 1C). The output ports of the two interferometers are imaged simultaneously on separate, vertically displaced cameras. A horizontal detection fringe (*13*) is applied to improve phase readout. As in (*13*), the direction of the detection fringe is reversed to suppress imaging-related systematic effects.

The source mass is a 170° semicircular ring with inner radius $R_y = 6.8$ cm, outer radius 7.8 cm, and height 3 cm, chosen to be consistent with apparatus geometric constraints. The ring has a mass of 1.25 kg and is 99.95% pure tungsten. We verified that the source mass is nonmagnetic at the level required for this work [see materials and methods for details (*15*)]. The mass is placed within the magnetic shield that surrounds the interferometry region at a height of 27 cm below the end cap. This position corresponds to $R_x = 0$, where R_x is the vertical displacement between the source mass and the apex of the upper arm trajectory.

In the phase shift plots of the $52\hbar k$ and $4\hbar k$ gradiometers as a function of R_x (Fig. 2), each data point represents the difference in the gradiometer phase with and without the source mass installed. This differential measurement technique suppresses the phase contribution from Earth's gravity gradient along with other systematic effects that are common to the two configurations.

The $4\hbar k$ interferometers have a small wave packet separation and can be understood as deflection measurements. This property enables a simple explanation of the shapes of the curves in Fig. 2B. At large approach distances ($R_x < 0, |R_x| \gg R_y$), all interferometers are far below the source mass, and the phase shifts are small. As the launch height is increased, the upper $4\hbar k$ interferometer approaches the source mass. The atoms are deflected upward toward the source mass, making the phase shift more negative. When $R_x > 0$, the atoms of the upper $4\hbar k$ interferometer spend time above the source mass and begin to be deflected downward by it; the phase shift thus passes through zero near $R_x = 4$ cm and becomes positive. At these approach distances, the atoms of the lower $4\hbar k$ interferometer begin to be deflected upward by the source mass, and the phase shift becomes negative. Unlike the upper $4\hbar k$ interferometer, the phase shift of the $52\hbar k$ interferometer remains negative for all values of R_x, indicating that it cannot be explained solely by deflections. The $52\hbar k$ gradiometer phase uncertainty in a single shot is typically about 30 mrad, inferred from the observed standard deviation of a sequence of shots.

To interpret our measurement as an Aharonov-Bohm experiment, we characterize the relationship between deflections, action differences, and the interferometer phase. The phase ϕ of a light-pulse matter-wave interferometer in a gravitational potential can be written as the sum of two terms: $\phi = \phi_{MP} + \phi_{\Delta S}$ (*12*). These terms have distinct physical interpretations. The "midpoint phase," ϕ_{MP}, arises from local atom-light interactions during beam splitter and mirror pulses (*11*, *12*). For a Bragg interferometer, the midpoint phase is expressed as $\phi_{MP} = -\sum_i k_i \cdot \bar{x}_i$, where k_i is the wave number difference applied to the two arms by the i^{th} light pulse and $\bar{x}_i$ is the midpoint displacement of the interferometer arms at the i^{th} light pulse with respect to the optical phase reference. Classically, the midpoint phase could be measured by observing the positions of particles that travel along the interferometer arm trajectories. By contrast, the beyond-midpoint phase is given by

$$\phi_{\Delta S} = \frac{\Delta S}{\hbar} = \frac{m}{\hbar}\int\left(\left[V(x_1,t) - V(x_2,t)\right] - \frac{\Delta x}{2}\left[\frac{\partial V(x_1,t)}{\partial x} + \frac{\partial V(x_2,t)}{\partial x}\right]\right) dt \quad (1)$$

for gravitational potential V, wave packet separation Δx, and arm trajectories $x_1(t)$, $x_2(t)$. The first term in the integrand depends on the potential energy difference between arms, whereas the second term depends on the kinetic energy difference. This phase is proportional to the proper time evolved around a closed interferometer loop. In principle, $\phi_{\Delta S}$ could be measured by observing the phase difference of two clocks with frequency mc^2/h that travel along the interferometer arms (*17*), but $\phi_{\Delta S}$ cannot be inferred by observing the interferometer arm trajectories. In previous gravitational measurements (*16*, *18*) and in our $4\hbar k$ gradiometers, $\phi_{\Delta S}$ is smaller than the measurement resolution.

In an ideal Aharonov-Bohm measurement, the interferometer arm trajectories would be completely unaltered by the potential. In that case, we would have $\frac{\partial V}{\partial x} = 0$ along both trajectories, $\phi_{MP} = 0$, and $\phi = \phi_{\Delta S} = \frac{m}{\hbar}\int[V(x_1,t) - V(x_2,t)]dt$. The same expression describes the phase in the originally proposed electric Aharonov-Bohm experiment (*1*), except that in the gravitational case, the phase is proportional to the mass rather than the electric charge. We therefore identify $\phi_{\Delta S}$ with ϕ_{AB}. In our measurement, the signal of interest is the gradiometer phase shift (the difference between the phase shifts of the upper and lower interferometers due to the source mass). There is no configuration in which the interferometer trajectories are completely unperturbed. However, there is a particular approach distance ($R_x = 6$ cm) at which the gradiometer phase response to the deflections sums to zero ($\phi_{MP} = 0$) and the kinetic energy

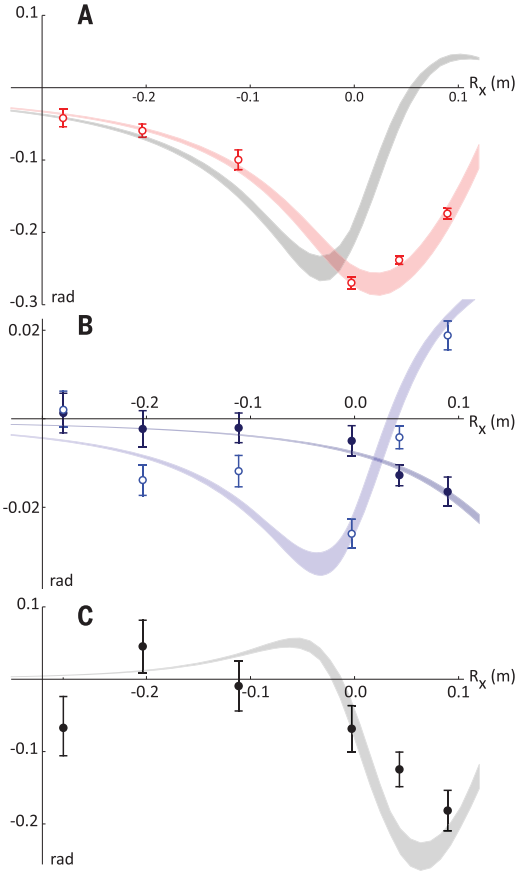

Fig. 2. Comparison of $52\hbar k$ and $4\hbar k$ gradiometers. (**A**) Phase shift induced by tungsten ring in $52\hbar k$ gradiometer as a function of R_x (red points). Theoretical predictions are based on quantum-mechanical calculation with semiclassical approximation (*12*) (red curve) and midpoint theorem (gray curve). The theoretical predictions are derived from ab initio models with no free parameters. Each point is the average of at least 20 shots; error bars and curve widths represent 1σ uncertainty. Curve widths are derived from uncertainty in source mass position. (**B**) Phase shifts of upper $4\hbar k$ gradiometer (light blue points) and lower $4\hbar k$ gradiometer (dark blue points) as a function of R_x, compared to theoretical predictions (light blue curve, dark blue curve). Each point is the average of at least 100 shots. (**C**) Beyond-midpoint phase shift $\phi_{\Delta S}$ of $52\hbar k$ gradiometer (black points) calculated from data in Figs. (A) and (B), compared to theoretical prediction (gray curve). $\phi_{\Delta S}$ differs significantly from zero at $R_x = 4$ cm and $R_x = 9$ cm.

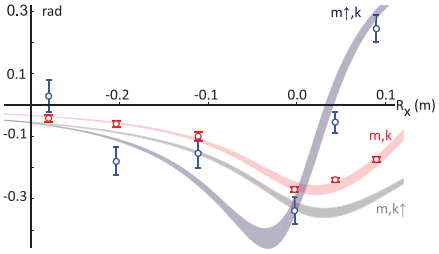

Fig. 3. Scaling properties of ϕ. Phase shift data (red points) and theoretical prediction (red curve) of $52\hbar k$ gradiometer as a function of R_x. Near $R_x = 0$, the measured phase shift comes within 20% of the prediction for the quantum limit (large k, $\Delta x/R \gg 1$) (gray curve). Because $V \sim -GmM/R$, the red data points remain negative for $R_x > 0$. The prediction for the classical limit (large m, $\Delta x/R \ll 1$) is given by the dark blue curve. This curve changes sign near $R_x = 0$. The phase shift of the upper $4\hbar k$ gradiometer (blue points), scaled by 52/4, agrees with the large-m curve. The large-k and large-m curves are calculated by keeping the uppermost arm trajectory and gradiometer baseline constant. Each red or blue point is the average of at least 20 or 100 shots, respectively; error bars and curve widths represent 1σ uncertainty.

contribution to the action difference also vanishes (*19*). Therefore, near $R_x = 6$ cm, the gradiometer phase shift is given by $\phi = \phi_{\Delta S} = \frac{m}{\hbar}\int[V(x_1,t) - V(x_2,t) - V(x_3,t) + V(x_4,t)]dt$ to within the experimental resolution, where x_3 and x_4 are the arm trajectories of the lower interferometer (*20*).

Together, the $4\hbar k$ gradiometers measure the midpoint phase term ϕ_{MP} of the $52\hbar k$ gradiometer (*15*). Specifically, $\phi_{MP} \approx \frac{52}{4}\cdot\frac{1}{2}(\phi_{upper} + \phi_{lower})$, where ϕ_{upper} and ϕ_{lower} are the phase shifts of the upper and lower $4\hbar k$ gradiometers, respectively. In Fig. 2C, we subtract the measured ϕ_{MP} from ϕ to construct $\phi_{\Delta S}$ for the $52\hbar k$ gradiometer. The signature of the Aharonov-Bohm effect is that $\phi_{\Delta S}$ is nonzero. The points at $R_x = 4$ cm (−125 ± 24 mrad) and $R_x = 9$ cm (−182 ± 28 mrad) differ significantly from zero, and the data set rejects the null hypothesis (no gravitational Aharonov-Bohm effect) with likelihood ratio 2×10^{-13}, corresponding to 7σ statistical significance. The uncertainties in Fig. 2C are limited primarily by the resolution of the $4\hbar k$ gradiometers. As shown in Fig. 2A, the phase shift of the $52\hbar k$ gradiometer differs from the theoretically predicted midpoint phase shift by 13σ at $R_x = 4$ cm and by 19σ at $R_x = 9$ cm. The $52\hbar k$ data are consistent with the full phase-shift prediction (reduced $\chi^2 = 0.6$).

In a weak gravitational potential, the midpoint phase term approximately cancels with the kinetic energy phase term [the second term in the integrand of Eq. 1; see supplementary text for details (*15*)]. We can therefore compute the interferometer phase shift due to the source mass as (*21*)

$$\phi = \frac{m}{\hbar}\int_0^{2T}[V(x_1,t) - V(x_2,t)]dt \qquad (2)$$

The scaling properties of ϕ depend on the ratio $\Delta x/R$ between the wave packet separation $\Delta x \propto \hbar k/m$ and the approach distance $R = \left(R_x^2 + R_y^2\right)^{1/2}$ between the upper arm and the source mass. As m is increased at constant k and R, $\Delta x/R \to 0$, and the phase shift

$$\phi \approx \frac{m}{\hbar}\int_0^{2T}\frac{\partial V}{\partial x}\cdot\Delta x dt = k\left[\int_0^T \frac{\partial V}{\partial x}t\,dt + \int_T^{2T}\frac{\partial V}{\partial x}(2T - t)dt\right] \qquad (3)$$

becomes linearly proportional to k and independent of m. In this classical regime where $\Delta S = 0$, the phase shift is proportional to the gravitational acceleration $\frac{\partial V}{\partial x}$ induced by the source mass and is equal to ϕ_{MP}. By contrast, as k is increased at constant m and R, the wave packet separation increases. As $\Delta x/R \to \infty$, the phase shift $\phi \approx \frac{m}{\hbar}\int V(x_1,t)dt$ becomes independent of k and depends linearly on m. In this quantum regime, the phase shift is proportional to the gravitational potential of the source mass. Figure 3 plots the phase shifts of the $52\hbar k$ and upper $4\hbar k$ gradiometers as a function of R_x, comparing them to the predictions for $\Delta x/R \ll 1$ and $\Delta x/R \gg 1$. The data for the upper $4\hbar k$ gradiometer are consistent with the classical limit.

The change in the scaling of ϕ from linear in k to linear in m is necessary to satisfy Heisenberg's error-disturbance relation, which was first introduced in Heisenberg's microscope thought experiment. This relation states that the maximum retrievable information in a quantum measurement is related to the amount of back-action it creates (*22*). The interferometer phase shift can be conceptualized as a measurement of the tungsten ring position R via the gravitational interaction $V \sim -GmM/R$, where M is the mass of the ring. The back-action of the atoms on the ring (i.e., the momentum recoil of the ring) is given by V and is proportional to m. Increasing the resolution of the interferometer by increasing k eventually saturates the retrievable information, as ϕ becomes insensitive to k and proportional to m, just like the back-action. Our data are consistent with Heisenberg's relation in the regime where one interaction partner is in a large quantum superposition.

The results obtained in this work are distinguished from previous gravitational measurements in quantum systems by the nonlocal nature of the observed phase shift. In prior experiments with freely falling (*18*) and guided (*23*) interferometers, the wave packet separation is small enough that the gravitational field is approximately uniform at the length scale of the interferometer. The interferometer is therefore a local system in the general-relativistic sense (*24*). According to the equivalence principle, it is not possible to observe gravitational effects in local systems. Such experiments test the equivalence principle but do not provide any further information about the interaction of gravity with quantum particles. In addition, our experiment operates in a different regime than the Pound-Rebka experiment (*25*, *26*), which measures the locally observable time dilation of displaced clocks due to nongravitational forces (*27*). The massive particles used in our interferometer measure the gravitationally induced time dilation along nonlocal trajectories, as observed in satellite experiments with classical clocks (*28*).

With a gravity gradient resolution of $5\times 10^{-10}/s^2$ per shot (differential acceleration resolution $1.1 \times 10^{-11}g$ per shot, $1.4 \times 10^{-12}g$ after 70 shots), the single-source gradiometer sets a new standard for ground-based gravity gradiometry (*16*) and could be incorporated into proposed space-based gradiometers (*29*). This result is the first observation of a gravitational phase shift that is intrinsically proportional to the mass of the test particle. In addition, the phase shift depends intrinsically on Planck's constant h and Newton's gravitational constant G. Combined with a precise characterization of the source mass, this interferometer could provide an improved measurement of G (*8*, *30*). These long-time, large-momentum-transfer interferometry techniques also enable more accurate tests of the equivalence principle (*13*), new searches for dark matter (*31*), and new types of gravitational-wave detectors (*32*).

REFERENCES AND NOTES

1. Y. Aharonov, D. Bohm, *Phys. Rev.* **123**, 1511–1524 (1959).
2. C. Marletto, V. Vedral, *Phys. Rev. Lett.* **125**, 040401 (2020).
3. R. G. Chambers, *Phys. Rev. Lett.* **5**, 3–5 (1960).
4. H. Batelaan, A. Tonomura, *Phys. Today* **62**, 38–43 (2009).
5. J. Gillot, S. Lepoutre, A. Gauguet, M. Büchner, J. Vigué, *Phys. Rev. Lett.* **111**, 030401 (2013).
6. J. Audretsch, C. Lammerzahl, *J. Phys. Math. Gen.* **16**, 2457–2477 (1983).
7. M. A. Hohensee, B. Estey, P. Hamilton, A. Zeilinger, H. Müller, *Phys. Rev. Lett.* **108**, 230404 (2012).
8. G. Rosi, F. Sorrentino, L. Cacciapuoti, M. Prevedelli, G. M. Tino, *Nature* **510**, 518–521 (2014).
9. P. Wolf *et al.*, *Class. Quantum Gravity* **28**, 145017 (2011).
10. Here and in the remainder of the text, ΔS is the gravitational contribution to the action difference. Action differences induced by photon recoil or by other electromagnetic interactions are not included.
11. C. Antoine, C. J. Bordé, *J. Opt. B Quantum Semiclassical Opt.* **5**, S199–S207 (2003).
12. C. Overstreet, P. Asenbaum, M. A. Kasevich, *Am. J. Phys.* **89**, 324–332 (2021).
13. P. Asenbaum, C. Overstreet, M. Kim, J. Curti, M. A. Kasevich, *Phys. Rev. Lett.* **125**, 191101 (2020).
14. M. Kim *et al.*, *Opt. Lett.* **45**, 6555–6558 (2020).

15. Materials and methods are available as supplementary materials.
16. P. Asenbaum *et al*., *Phys. Rev. Lett.* **118**, 183602 (2017).
17. Although the interferometer phase is sensitive to the proper time difference between arms, the interferometer does not produce any signal at the Compton frequency mc^2/h. Our measurement does not test the universality of gravitational redshift (*26*).
18. R. Colella, A. W. Overhauser, S. A. Werner, *Phys. Rev. Lett.* **34**, 1472–1474 (1975).
19. The tungsten ring changes the velocity of the atoms on the order of 1 nm/s, which is seven orders of magnitude smaller than the recoil velocity from the interferometer beam splitters. Therefore, quadratic terms in the deflection velocity are negligible. See supplementary text for details (*15*).
20. Note that this condition is achieved even though the source mass is stationary in the reference frame of the laboratory.
21. P. Storey, C. Cohen-Tannoudji, *J. Phys. II* **4**, 1999–2027 (1994).
22. P. Busch, P. Lahti, R. F. Werner, *Phys. Rev. Lett.* **111**, 160405 (2013).
23. V. Xu *et al*., *Science* **366**, 745–749 (2019).
24. We use "local" to describe systems in which the length scale is small enough, and the measurement sensitivity low enough, that the effects of gravitational curvature are negligible.
25. R. V. Pound, G. A. Rebka, *Phys. Rev. Lett.* **4**, 337–341 (1960).
26. A. Roura, *Phys. Rev. X* **10**, 021014 (2020).
27. C. M. Will, *Living Rev. Relativ.* **17**, 4 (2014).
28. R. F. C. Vessot *et al*., *Phys. Rev. Lett.* **45**, 2081–2084 (1980).
29. O. Carraz, C. Siemes, L. Massotti, R. Haagmans, P. Silvestrin, *Microgravity Sci. Technol.* **26**, 139–145 (2014).
30. H. Müller, in *Atom Interferometry*, G. M. Tino, M. A. Kasevich, Eds. (Amsterdam, Bologna: IOS Press and SIF, 2014), pp. 389-390.
31. A. Arvanitaki, P. W. Graham, J. M. Hogan, S. Rajendran, K. Van Tilburg, *Phys. Rev. D* **97**, 075020 (2018).
32. M. Abe *et al*., *Quantum Sci. Technol.* **6**, 044003 (2021).
33. C. Overstreet, P. Asenbaum, J. Curti, M. Kim, M. A. Kasevich, Replication Data for: Observation of a gravitational Aharonov-Bohm effect, Harvard Dataverse, V2 (2021); https://doi.org/10.7910/DVN/O9IS7Y.

ACKNOWLEDGMENTS

We thank T. Kovachy, T. Hensel, and M. Aspelmeyer for fruitful discussions. **Funding:** We acknowledge funding from the Defense Threat Reduction Agency, the Office of Naval Research, and the Vannevar Bush Faculty Fellowship program. M. K. acknowledges funding from the Kwanjeong Educational Foundation. **Author contributions:** C.O. and P.A. designed the experiment. C.O., P.A., J.C., and M.K. carried out the experiments. C.O., P.A., and M.A.K. analyzed the results. **Competing interests:** M.A.K. serves as Chief Scientist (consulting) for AOSense, Inc. **Data and materials availability:** The data are available at Harvard Dataverse (*33*).

SUPPLEMENTARY MATERIALS

science.org/doi/10.1126/science.abl7152
Materials and Methods
Supplementary Text
Figs. S1 and S2
References (*34*, *35*)

30 July 2021; accepted 16 November 2021
10.1126/science.abl7152

Science

Observation of a gravitational Aharonov-Bohm effect

Chris OverstreetPeter AsenbaumJoseph CurtiMinjeong KimMark A. Kasevich

Science, 375 (6577), • DOI: 10.1126/science.abl7152

Gravitational interference

The Aharonov-Bohm effect is a quantum mechanical effect in which a magnetic field affects the phase of an electron wave as it propagates along a wire. Atom interferometry exploits the wave characteristic of atoms to measure tiny differences in phase as they take different paths through the arms of an interferometer. Overstreet *et al*. split a cloud of cold rubidium atoms into two atomic wave packets about 25 centimeters apart and subjected one of the wave packets to gravitational interaction with a large mass (see the Perspective by Roura). The authors state that the observed phase shift is consistent with a gravitational Aharonov-Bohm effect. —ISO

Science (ISSN) is published by the American Association for the Advancement of Science. 1200 New York Avenue NW, Washington, DC 20005. The title *Science* is a registered trademark of AAAS.